



Abnormal blue-shift of Eu^{2+} -activated calcium zirconium phosphates $\text{CaZr}_4(\text{PO}_4)_6$

Zhi-Jun Zhang, Woochul Yang*

Department of Physics, Dongguk University, Pildong-ro, Choong-gu, Seoul 100-715, South Korea



ARTICLE INFO

Article history:

Received 28 March 2015

Received in revised form 27 April 2015

Accepted 6 May 2015

Available online 3 June 2015

Keywords:

Eu^{2+}

Phosphate

Luminescence

Blue shift

ABSTRACT

The electronic structure of $\text{CaZr}_4(\text{PO}_4)_6$ was calculated using the CASTEP code and the band gap for $\text{CaZr}_4(\text{PO}_4)_6$ can reach up to 4.30 eV. $\text{Ca}_{1-x}\text{Eu}_x\text{Zr}_4(\text{PO}_4)_6$ ($0.01 \leq x \leq 1$) samples were prepared by a high temperature solid-state reaction method. XRD analysis shows that Eu^{2+} ion can be totally incorporated into $\text{CaZr}_4(\text{PO}_4)_6$ forming complete solid solutions with trigonal lattice. $\text{Ca}_{1-x}\text{Eu}_x\text{Zr}_4(\text{PO}_4)_6$ ($0.01 \leq x \leq 1$) shows typical broad band emission in wavelength range from 400 to 650 nm for both under ultraviolet (UV) light and X-ray excitation, originating from the $4f^65d^1 \rightarrow 4f^75d^0$ transition of Eu^{2+} ions. With increasing Eu^{2+} concentration, there is abnormal blue-shift of the emission peaks for $\text{Ca}_{1-x}\text{Eu}_x\text{Zr}_4(\text{PO}_4)_6$ due to the decreasing crystal field strength and Stokes shift. With increasing temperature in $\text{CaZr}_4(\text{PO}_4)_6: \text{Eu}^{2+}$, its emission bands show the anomalous blue-shift with decreasing intensity. The overall scintillation efficiency of $\text{Ca}_{0.9}\text{Eu}_{0.1}\text{Zr}_4(\text{PO}_4)_6$ is 1.7 times of that of $\text{Bi}_4\text{Ge}_3\text{O}_{12}$ (BGO) powder under the same conditions. In addition, its predominant decay time is about 50 ns at room temperature. The potential application of Eu^{2+} -doped $\text{CaZr}_4(\text{PO}_4)_6$ has been pointed out.

© 2015 Elsevier B.V. All rights reserved.

1. Introduction

Rare-earth activated inorganic luminescent materials with wide band gap have been widely used in diverse applications, such as scintillation, X-ray imaging, mercury-free lamps and color display [1]. Among these inorganic phosphors, Eu^{2+} activated phosphors have been studied intensely since the broad band characteristics of emission and excitation spectra of Eu^{2+} , originating from the transition between the $^8\text{S}_{7/2}$ ($4f^7$) ground state and the $4f^65d^1$ excited state configuration. The position of the 5d energy levels strongly depends on the local environment of Eu^{2+} , such as covalence and crystal field splitting, in the specific host lattice. Furthermore, the 5d–4f transition of Eu^{2+} decays relatively fast, making the Eu^{2+} -activated materials to be used as potential scintillator [2,3]. Therefore, in the last decade, designing and developing new Eu^{2+} activated phosphors for X-ray or light emitting diode (LED) have been boosted by the rapid development of the related industries around the world [4–6].

During the past few years, zirconium-based phosphates have attracted enormous attention and have been extensively investigated, since many of these compounds not only have been explored as catalysts and ion exchanger, but also as host materials

for the X-ray and LED phosphors [7,8]. Recently, calcium zirconium phosphate, $\text{CaZr}_4(\text{PO}_4)_6$ has been investigated for its potential applications as ion exchangers and host material for radioactive waste immobilization, $\text{CaZr}_4(\text{PO}_4)_6$ has the structural flexibility with respect to isomorphous ionic replacement and high stability against leaching reactions [9]. In addition, because of their very low coefficient and anisotropy of thermal expansion, low thermal conductivity, as well as high temperature stability, making them as attractive materials for oxidation resistant coating applications on carbon–carbon composites [10,11]. The crystal structure of $\text{CaZr}_4(\text{PO}_4)_6$ is understood in terms of PO_4 tetrahedra and ZrO_6 octahedra which are linked at the corners around c axis forming a three-dimensional network, and a three-dimensionally linked interstitial space is occupied partially by Ca^{2+} ions [9]. More importantly, the existence of octahedral $\text{Zr}(\text{PO}_4)_6$ moiety as an efficient luminescence center in the crystal structures of $\text{CaZr}_4(\text{PO}_4)_6$, makes them as good host lattices for potential applications for X-ray or LED phosphor. The spectroscopic properties of trivalent rare-earth ions (Sm^{3+} , Tb^{3+} , Dy^{3+}) in $\text{CaZr}_4(\text{PO}_4)_6$ in the vacuum ultraviolet–ultraviolet (VUV–UV) range have been systematically investigated to explore the potential for use as phosphors for plasma display panels (PDP) [12] or near ultraviolet white light emitting diodes (NUVLED) [13]. Hirayama has reported the luminescence properties of divalent Eu in $\text{CaZr}_4(\text{PO}_4)_6$ prepared by co-precipitation method in the reduction atmosphere [14]. In

* Corresponding author.

E-mail address: wyang@dongguk.edu (W. Yang).

addition, several methods, such as electron spin resonance (ESR), X-ray photoelectron spectroscopy (XPS), etc. were employed to investigate the valence state of Eu in $\text{CaZr}_4(\text{PO}_4)_6$ prepared in air atmosphere [15]. Different from the previous reported work, in this paper, we focus on the electronic structure of $\text{CaZr}_4(\text{PO}_4)_6$, the effect of Eu^{2+} concentration in $\text{CaZr}_4(\text{PO}_4)_6$ on the crystal structure, UV and X-ray excited luminescence properties, as well as the fluorescence decay time will be studied in detail, and explore their potential possibilities to be used as a new kind of blue-emitting phosphors for LED or X-ray imaging.

2. Experimental section

2.1. Samples preparation

$\text{Ca}_{1-x}\text{Eu}_x\text{Zr}_4(\text{PO}_4)_6$ ($0.01 \leq x \leq 1$) powder samples were prepared by solid-state reactions at high temperature. The starting materials, CaCO_3 , ZrO_2 , $\text{NH}_4\text{H}_2\text{PO}_4$ and Eu_2O_3 , were analytical grade (99.99% purity) without further purification. Stoichiometric amounts of CaCO_3 , ZrO_2 , $\text{NH}_4\text{H}_2\text{PO}_4$ and Eu_2O_3 were thoroughly mixed and preheated at 200°C for 2 h to decompose the $\text{NH}_4\text{H}_2\text{PO}_4$, then pre-sintered at 800°C for 2 h to decompose CaCO_3 , finally and re-sintered at 1300°C for 5 h under $\text{N}_2\text{-H}_2$ (5%) atmosphere to transform any meta-phosphate to orthophosphate. After firing, these samples were gradually cooled down to room temperature in the furnace.

2.2. Characterizations

The X-ray diffraction (XRD) data for phase identification and index were collected at ambient temperature with a HUBER Imaging Plate Guinier Camera G670 [S] ($\text{Cu } K_{\alpha 1}$ radiation, $\lambda = 1.54056 \text{ \AA}$, Ge monochromator). The 2θ ranges of all the data sets are from 5° to 100° with a step of 0.005° . The unit cells of $\text{Ca}_{1-x}\text{Eu}_x\text{Zr}_4(\text{PO}_4)_6$ ($0.01 \leq x \leq 1$) were determined from the X-ray powder diffraction patterns using the indexing program Fullprof [16]. The diffuse reflectance spectra in the UV and visible range were recorded using Cary 5000 spectrophotometer (Varian Inc., USA) with a Xe flash lamp. The X-ray excited luminescence (XEL) of the samples was examined under room temperature using an X-ray excited spectrometer (Fluormain), in which an F-30 X-ray tube (W anticathode target) was used as the X-ray source operating at a peak voltage of 30 kV and a peak current of 4 mA. UV excitation and emission spectra, as well as the temperature-depend emission spectra were measured using Hitachi F-4600 spectrometer. The scan speed was fixed at 240 nm/min, the voltage was 400 V and the slits were fixed at 2.5 nm. The transient decays were recorded on an Edinburgh Instruments (FLS920) spectrofluorimeter equipped with both continuous (450 W) and pulsed Xe lamps. All of the luminescence spectra were recorded at room temperature.

2.3. Electronic structure calculation

The electronic structure calculation of undoped $\text{CaZr}_4(\text{PO}_4)_6$ was carried out by using the CASTEP code which utilizes pseudopotential to describe electron-ion interactions and represents electronic wave functions by means of a plane-wave basis set. Perdew-Burke-Ernzerhof (PBE) functional within generalized gradient approximation (GGA) was adopted for the theoretical basis of density function. Two steps were necessary for calculating the electronic band structures of $\text{CaZr}_4(\text{PO}_4)_6$. The first step was to optimize its crystal structure using the crystallographic data reported in the literature [9]. There was only a small difference between the experimental unit cell parameters and the calculated

ones after crystal structure optimization. The second step was to calculate the band structure and density of states of $\text{CaZr}_4(\text{PO}_4)_6$, based on the lattice parameters and atom coordinates fixed at the values obtained by the crystal structure optimization process. For the two steps, the following basic parameters were chosen in the setting up CASTEP: the kinetic energy cutoff is 550 eV, k -point spacing is 0.04 \AA^{-1} , sets of k -points is $4 \times 4 \times 4$, self-consistent field (SCF) tolerance thresholds is 5.0×10^{-7} eV per atom, and the space representation is reciprocal.

3. Results and discussion

3.1. The electronic structure of $\text{CaZr}_4(\text{PO}_4)_6$

Fig. 1(a) shows the band structure of $\text{CaZr}_4(\text{PO}_4)_6$ calculated by using CASTEP code, respectively. $\text{CaZr}_4(\text{PO}_4)_6$ exhibits an indirect band gap, and the value of its band gap between the lowest energy of conduction bands (CBs) and highest energy of valence bands (VBs) is about 4.30 eV. The generalized gradient approximation used in density functional theory does not accurately describe the eigenvalues of the electronic states [17], as a consequence, the value of the calculated band gap is underestimated compared with the experimental results (5.01 eV as shown in Section 3.3). The large band gap of the host materials helps to locate both the ground and excited states of the luminescent activators within

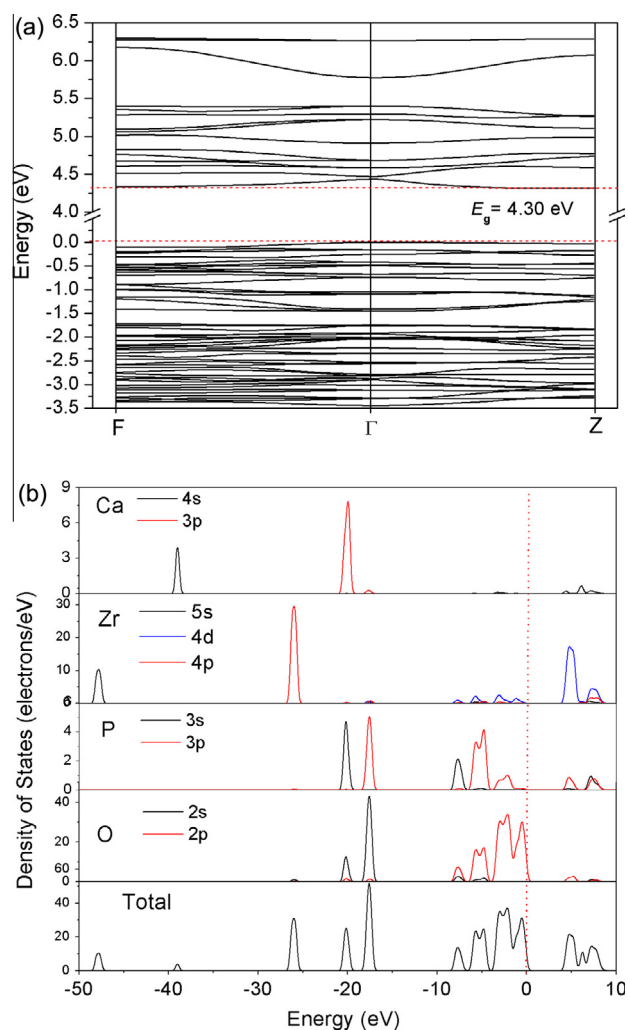


Fig. 1. Band structure (a), total and partial density of states (b) of $\text{CaZr}_4(\text{PO}_4)_6$.

Download English Version:

<https://daneshyari.com/en/article/1493701>

Download Persian Version:

<https://daneshyari.com/article/1493701>

[Daneshyari.com](https://daneshyari.com)